

A crossed molecular beams study on the formation and energetics of the resonantly stabilized free $i\text{-C}_4\text{H}_3(\text{X}^2\text{A}')$ radical and its isotopomers

Xibin Gu ^a, Ying Guo ^a, Fangtong Zhang ^a, Alexander M. Mebel ^b, Ralf I. Kaiser ^{a,*}

^a Department of Chemistry, University of Hawai'i at Manoa, Honolulu, HI 96822, United States

^b Department of Chemistry and Biochemistry, Florida International University, Miami, FL 33199, United States

Received 23 November 2006; accepted 27 March 2007

Available online 18 April 2007

Abstract

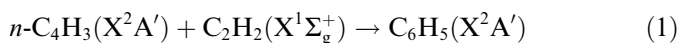
The chemical dynamics of the formation of the $i\text{-C}_4\text{H}_3(\text{X}^2\text{A}')$ radical together with its partially deuterated isotopomers were investigated in eight crossed molecular beams experiments of dicarbon molecules in their $\text{X}^1\Sigma_g^+$ electronic ground and in first excited $\text{a}^3\Pi_u$ state with (partially deuterated) ethylene at collision energies between 12.1 and 40.9 kJ mol⁻¹. The center-of-mass angular distributions suggest that the reaction dynamics on the singlet and triplet surfaces are indirect and involve butatriene reaction intermediates. In case of the $\text{C}_2/\text{C}_2\text{H}_4$ reaction, the 'symmetric' singlet butatriene intermediate would lead solely to a symmetric center-of-mass angular distribution; however, in combination with isotopically labeled reactants, we deduced that triplet butatriene intermediates excited to B/C like rotations likely account for the observed asymmetries in the center-of-mass angular distributions at higher collision energies. The translational energy distributions are also indicative of the involvement of both the triplet and singlet surfaces which lead both to the $i\text{-C}_4\text{H}_3(\text{X}^2\text{A}')$ radicals through loose (singlet) and tight (triplet) exit transition states. Also, our experiments helped to determine the enthalpy of formation of the $i\text{-C}_4\text{H}_3(\text{X}^2\text{A}')$ radical to be about 504 ± 10 kJ mol⁻¹ in good agreement with previous computational studies suggesting 498–499 kJ mol⁻¹. The explicit identification of the resonance-stabilized $i\text{-C}_4\text{H}_3(\text{X}^2\text{A}')$ radical proposes that the reaction of dicarbon with ethylene can lead to formation of $i\text{-C}_4\text{H}_3(\text{X}^2\text{A}')$ in combustion flames; the $n\text{-C}_4\text{H}_3(\text{X}^2\text{A}')$ isomer is not formed in this reaction. This conclusion correlates nicely with Hansen's et al. flame experiments at the advanced light source observing only the $i\text{-C}_4\text{H}_3(\text{X}^2\text{A}')$ radical in hydrocarbon flames.

Published by Elsevier B.V.

Keywords: Combustion chemistry; Reaction dynamics; Crossed beams; Hydrocarbon radicals; Dicarbon

1. Introduction

Small, resonantly stabilized free hydrocarbon radicals have been proposed to be involved in the formation of the first aromatic ring species in combustion flames [1–6] and in the preparation of carbon–carbon composites [7]. Here, the reaction of the $n\text{-C}_4\text{H}_3$ radical (HCCHCCH) with acetylene (C_2H_2) is thought to lead to the synthesis of the first six-membered aromatic ring in combustion flames, i.e. the phenyl radical (C_6H_5 ; reaction (1)) [4,8,9]



A recent theoretical study by Mebel et al. suggested that reaction intermediates on the C_6H_6 potential energy surface can be either stabilized, isomerize prior to their stabilization to acyclic structures and/or benzene, or fragment via atomic and/or molecular hydrogen loss forming C_6H_5 isomers such as the phenyl radical and C_6H_4 structures like *o*, *m*, *p*-didehydrobenzenes [10]. The authors suggested also the formation of lower mass fragments such as the $n/i\text{-C}_4\text{H}_3 + \text{C}_2\text{H}_3$, channel involving not only the $n\text{-C}_4\text{H}_3$ radical, but also its $i\text{-C}_4\text{H}_3$ isomer (H_2CCCCH ; $\text{X}^2\text{A}'$) (Fig. 1). Both the $i\text{-C}_4\text{H}_3(\text{X}^2\text{A}')$ and the $n\text{-C}_4\text{H}_3(\text{X}^2\text{A}')$ radicals can be interconverted via atomic hydrogen elimination–addition reactions involving diacetylene (HCCCCH) [11]. The barrier of a hydrogen atom addition to the C2 position of diacetylene forming the $n\text{-C}_4\text{H}_3$

* Corresponding author.

E-mail address: kaiser@gold.chem.hawaii.edu (R.I. Kaiser).

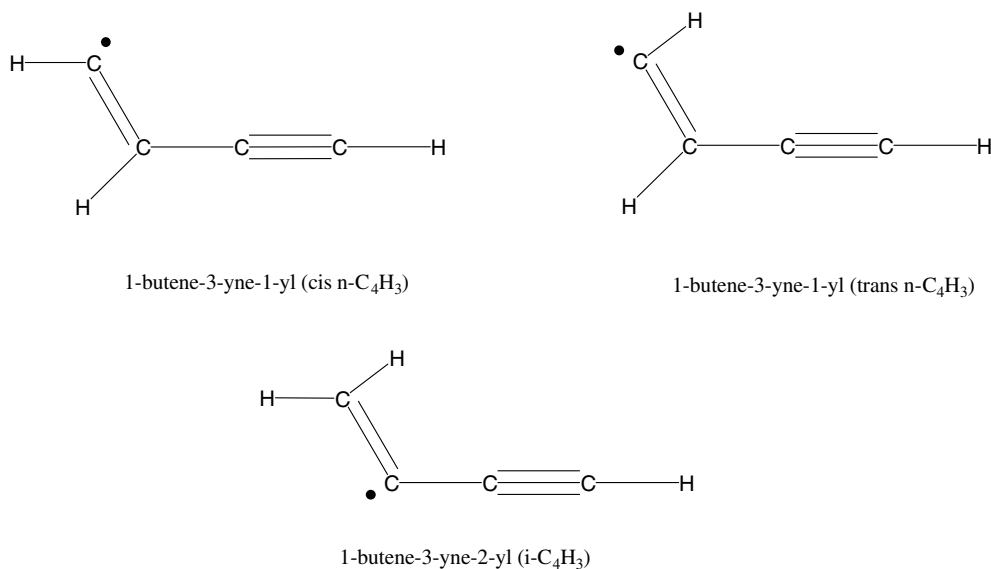


Fig. 1. Structures of the *cis/trans* $n\text{-C}_4\text{H}_3$ isomers (top) and the $i\text{-C}_4\text{H}_3$ (bottom).

radical was found to be 28.5 kJ mol^{-1} – higher by about 16 kJ mol^{-1} as that involved in the addition to the terminal carbon atom of the diacetylene molecule leading to the $i\text{-C}_4\text{H}_3$ isomer. Note that Hansen et al. explicitly observed the $i\text{-C}_4\text{H}_3(X^2A')$ radical in hydrocarbon flames. Based on the ionization potential of $8.06 \pm 0.05 \text{ eV}$, the authors derived an enthalpy of formation of $498 \pm 4 \text{ kJ mol}^{-1}$ at 0 K; this value corresponds nicely with computed enthalpies of formation of $499.4 \text{ kJ mol}^{-1}$ (298 K) [11], $499.8 \text{ kJ mol}^{-1}$ (298 K) [12], and $498.1 \text{ kJ mol}^{-1}$ (0 K) [13]. The corresponding $n\text{-C}_4\text{H}_3(X^2A')$ isomer, which is thermodynamically less stable by $27.6\text{--}48.1 \text{ kJ mol}^{-1}$ [11–13] was not observed [14]. Recall that the $i\text{-C}_4\text{H}_3(X^2A')$ radical has been observed as a product of the reaction of atomic carbon, $\text{C}(^3P_j)$, with allene (H_2CCCH_2) [15] and methylacetylene (CH_3CCH) [16] under single collision conditions. Both the $n\text{-C}_4\text{H}_3$ and $i\text{-C}_4\text{H}_3$ isomers have also been inferred as intermediates in the reactions of the ethynyl radical (C_2H) with acetylene [17]; bimolecular collisions of carbon atoms, $\text{C}(^3P_j)$, with the propargyl radical (C_3H_3) involve the unimolecular decomposition of the $i\text{-C}_4\text{H}_3$ structure [18]. Finally, recent crossed beams [19,20] and theoretical studies [21] of the reactions of ground and excited state dicarbon molecules, $\text{C}_2(X^1\Sigma_g^+/a^3\Pi_u)$, with ethylene (C_2H_4) also suggested that $i\text{-C}_4\text{H}_3$ can be formed on the singlet and triplet potential energy surfaces, respectively.

However, several features of this reaction have remained hard to pin down so far. First, the previous crossed beams experiments were carried out at a relatively low signal to noise ratio of only 7:1 [19]; this could prevent the identification of the molecular hydrogen elimination channel which electronic structure calculations predicted to exist on the singlet surface [21]. Secondly, the relative importance of the singlet versus triplet surfaces remains to be ascertained. Thirdly, we would like to determine experimentally the enthalpy of formation of the $i\text{-C}_4\text{H}_3(X^2A')$ radical and com-

pare our value with Hansen's data [14]. Finally, our previous investigation could not distinguish to what extent the forward–backward symmetric angular distributions originating from the decomposition of the singlet butatriene intermediates were the result of a long-lived complex or the consequence of a 'symmetric' intermediate (D_{2h}). Here, a 'symmetric intermediate' is defined as a decomposing molecule in which a leaving hydrogen atom can be inter converted by a twofold rotation axis with an equal probability of the hydrogen atom leaving in a direction of θ° or $\pi-\theta^\circ$; as a result, the center-of-mass angular distribution is forward–backward symmetric although the life-time of the intermediate might be less than its rotation period [22].

To shed light on these open questions, we expanded our previous studies and investigated the collision-energy dependent chemical dynamics of the reaction between dicarbon molecules in their $X^1\Sigma_g^+$ and $a^3\Pi_u$ electronic states with ethylene, $\text{C}_2\text{H}_4(X^1A_g)$, at four collision energies between 12.1 kJ mol^{-1} and 40.9 kJ mol^{-1} . Here, the collision-energy dependence of the center-of-mass angular distributions is anticipated to gain insights on the involvement of the singlet versus triplet surface. Also, we conducted the reaction with partially deuterated reactants, i.e. $\text{C}_2\text{H}_3\text{D}(X^1A')$, at a selected collision energy of 12.3 kJ mol^{-1} to reduce the symmetry of the singlet butatriene intermediate from D_{2h} to C_s . This is expected to help elucidating to what extent the forward–backward symmetric center-of-mass angular distribution is the effect of the symmetry of the butatriene intermediate or solely from a long-lived complex behavior. Thirdly, crossed beams experiments with three D_2 -ethylene isotopomers, i.e. $\text{H}_2\text{CCD}_2(X^1A_1)$, $\text{trans-C}_2\text{H}_2\text{D}_2(X^1A_1)$, and $\text{cis-C}_2\text{H}_2\text{D}_2(X^1A_1)$, were conducted to investigate the influence of the deuterium substitution and hence reduced symmetry on distinct rotational axis of the decomposing complex(es). Finally, we carried out experiments with $\text{C}_2\text{D}_4(X^1A_g)$ to

compare the life time(s) of the perdeuterated C_4D_4 isotopomers with the corresponding C_4H_4 molecules.

2. Experimental setup and data analysis

The experiments were performed under single collision conditions in a crossed molecular beams machine at The University of Hawai'i [23]. Pulsed dicarbon beams were produced in the primary source by laser ablation of graphite at 266 nm [24] (30 Hz). The ablated species were seeded in neat carrier gas (neon and helium; 99.9999%; 4 atm) released by a Proch-Trickl pulsed valve. After passing a skimmer, a four-slot chopper wheel selected a part out of the dicarbon beam at a peak velocities v_p between $1041 \pm 9 \text{ ms}^{-1}$ and $2353 \pm 96 \text{ ms}^{-1}$ (Table 1); at these velocities, the beam contains dicarbon in its $X^1\Sigma_g^+$ electronic ground and in its first excited $a^3\Pi_u$ state [23,25]; the energy separation between both states is only 8.6 kJ mol^{-1} . The segments of the dicarbon beam crossed a pulsed, (isotopically substituted) ethylene beam released by a second pulsed valve perpendicularly under well-defined collision energies between $12.1 \pm 0.1 \text{ kJ mol}^{-1}$ and $40.9 \pm 3.0 \text{ kJ mol}^{-1}$ in the interaction region (Table 1). The ablation beam contains also carbon atoms and tricarbon molecules. However, the latter do not interfere with the scattering signal of the dicarbon-ethylene reaction at mass-to-charge ratios (m/z) of 51 ($C_4H_3^+$)–48 (C_4^+). Tricarbon was found to react with ethylene only at collision energies larger than $42 \pm 4 \text{ kJ mol}^{-1}$ [26]. Signal from the reaction of atomic carbon with ethylene gives signal at m/z values of 39 ($C_3H_3^+$) and lower [27].

The reactively scattered species are monitored using a quadrupole mass spectrometric detector in the time-of-flight (TOF) mode after electron-impact ionization of the molecules. This detector can be rotated within the plane defined by the primary and the secondary reactant beams

Table 1

Peak velocities (v_p), speed ratios (S), center-of-mass angles (Θ_{CM}), together with the nominal collision energies of the dicarbon and the ethylene reactants (E_c)

Beam	v_p (ms^{-1})	S	E_c , kJ mol^{-1}	Θ_{CM}
$C_2H_4(X^1A_g)$	893 ± 3	15.7 ± 1.0	–	–
$C_2(X^1\Sigma_g^+/a^3\Pi_u)/Ne$	1041 ± 9	5.7 ± 0.2	12.1 ± 0.1	44.9 ± 0.3
$C_2(X^1\Sigma_g^+/a^3\Pi_u)/Ne$	1513 ± 25	3.4 ± 0.1	19.9 ± 0.5	34.5 ± 0.5
$C_2(X^1\Sigma_g^+/a^3\Pi_u)/He$	1966 ± 22	5.5 ± 0.2	30.1 ± 0.6	27.8 ± 0.3
$C_2(X^1\Sigma_g^+/a^3\Pi_u)/He$	2353 ± 96	3.6 ± 0.3	40.9 ± 3.0	23.8 ± 0.9
$C_2H_3D(X^1A')$	880 ± 3	15.6 ± 1.0	–	–
$C_2(X^1\Sigma_g^+/a^3\Pi_u)/Ne$	1045 ± 5	5.1 ± 0.1	12.3 ± 0.1	45.5 ± 0.2
$H_2CCD_2(X^1A_1)$	878 ± 3	15.5 ± 1.0	–	–
$C_2(X^1\Sigma_g^+/a^3\Pi_u)/He$	1942 ± 11	4.6 ± 0.1	30.3 ± 0.3	29.5 ± 0.3
$trans\text{-}C_2H_2D_2(X^1A_1)$	878 ± 3	15.5 ± 1.0	–	–
$C_2(X^1\Sigma_g^+/a^3\Pi_u)/He$	1975 ± 12	4.4 ± 0.1	31.2 ± 0.3	29.1 ± 0.2
$cis\text{-}C_2H_2D_2(X^1A_1)$	878 ± 3	15.5 ± 1.0	–	–
$C_2(X^1\Sigma_g^+/a^3\Pi_u)/He$	1974 ± 9	4.4 ± 0.1	31.1 ± 0.3	29.1 ± 0.2
$C_2D_4(X^1A_g)$	876 ± 3	15.4 ± 1.0	–	–
$C_2(X^1\Sigma_g^+/a^3\Pi_u)/He$	1941 ± 3	4.2 ± 0.1	31.1 ± 0.1	31.2 ± 0.1

to take angular resolved TOF spectra. By integrating the TOF spectra at distinct laboratory angles, we obtain the laboratory angular distribution, i.e. the integrated signal intensity of an ion of distinct m/z versus the laboratory angle. Information on the chemical dynamics was extracted by fitting these TOF spectra and the angular distribution in the laboratory frame (LAB) using a forward-convolution routine. [28] This approach initially assumes an angular distribution $T(\theta)$ and a translational energy distribution $P(E_T)$ in the center-of-mass reference frame (CM). TOF spectra and the laboratory angular distribution were then calculated from these center-of-mass functions. The final outcome is the generation of a product flux contour map which reports the differential cross section, $I(\theta, u)$, of the product as the intensity as a function of angle θ and product center-of-mass velocity u . This map contains all the details of the scattering process.

3. Results

3.1. Reactive scattering signal and TOF spectra

3.1.1. The $C_2(X^1\Sigma_g^+/a^3\Pi_u)/C_2H_4$ System

Reactive scattering signal was observed at mass-to-charge ratios, m/z , of 51 ($C_4H_3^+$), 50 ($C_4H_2^+$), 49 (C_4H^+), and 48 (C_4^+). We would like to stress that at each collision energy, the TOF spectra recorded at mass-to-charge ratios between 51 and 48 are super-imposable. This shows that the C_4H_3 molecule formed undergoes electron-impact induced fragmentation in the electron impact ionizer to $m/z = 50, 49$, and 48. Secondly, this finding demonstrates that only the dicarbon versus atomic hydrogen channel is observed in the experiments. We also detected ions at lower mass-to-charge ratios of 39 ($C_3H_3^+$), 38 ($C_3H_2^+$), and 37 (C_3H^+). TOF of these ions had to be fit with two channels, i.e. one pathway from fragmentation of the C_4H_3 radical in the electron impact ionizer and a second channel from the propargyl radical ($m/z = 39$) and its fragments at $m/z = 38$ and 37 [29]. Recall that the propargyl radical is formed in the bimolecular reaction of atomic carbon with ethylene as investigated earlier [27]. Finally, signal at $m/z = 36$ (C_3^+) has contributions from three channels. These were fragmentation of C_4H_3 and C_3H_3 in the electron impact ionizer (channels 1 and 2) and inelastically scattered tricarbon molecules [29]. The TOF data and laboratory angular distributions of the most intense m/z fragment, i.e. $m/z = 50$ ($C_4H_2^+$) are displayed in Figs. 2a and 3a, respectively. Summarized, the interpretation of the TOF data and LAB distributions verifies the presence of a dicarbon versus atomic hydrogen exchange channel leading to C_4H_3 isomer(s) under single collision conditions at each collision energy.

3.2. The $C_2(X^1\Sigma_g^+/a^3\Pi_u)/C_2H_3D$ / *cis, trans, gem-C₂H₂D₂* / C_2D_4 systems

To obtain additional information on the reaction dynamics, we also conducted experiments with D1-ethylene

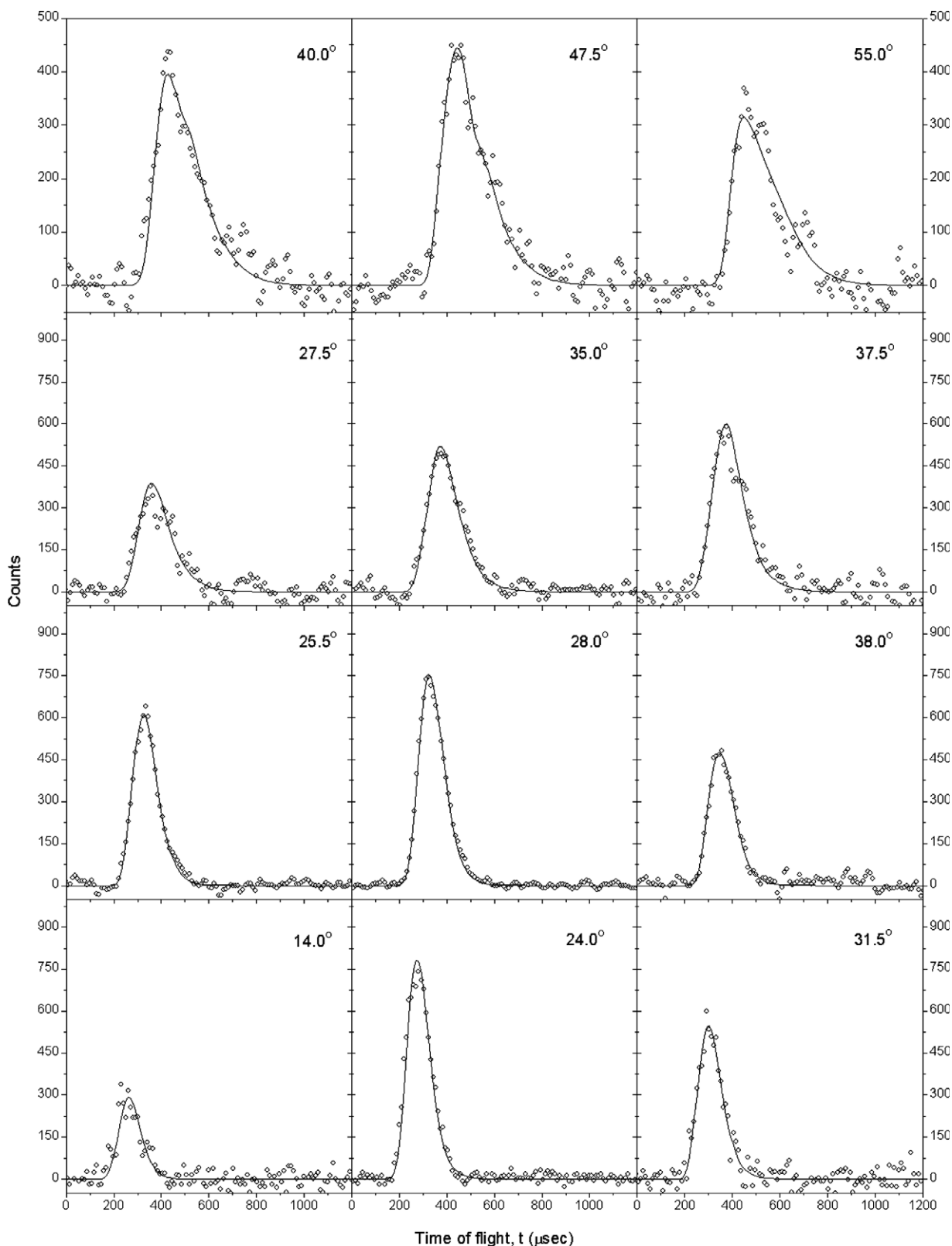


Fig. 2a. Selected time-of-flight data for $m/z = 50$ ($C_4H_2^+$) recorded at four collision energies of 12.1, 19.9, 30.1, and 40.9 kJ mol^{-1} (top row to bottom row) at various laboratory angles for the reaction of dicarbon molecules with ethylene. The circles indicate the experimental data, the solid lines the calculated fits.

($C_2H_3D(X^1A')$) at a selected collision energy of 12.3 kJ mol^{-1} (recall that this experiment was aimed to

reduce the symmetry of the singlet butatriene intermediate to C_s). In addition, crossed beams experiments with three

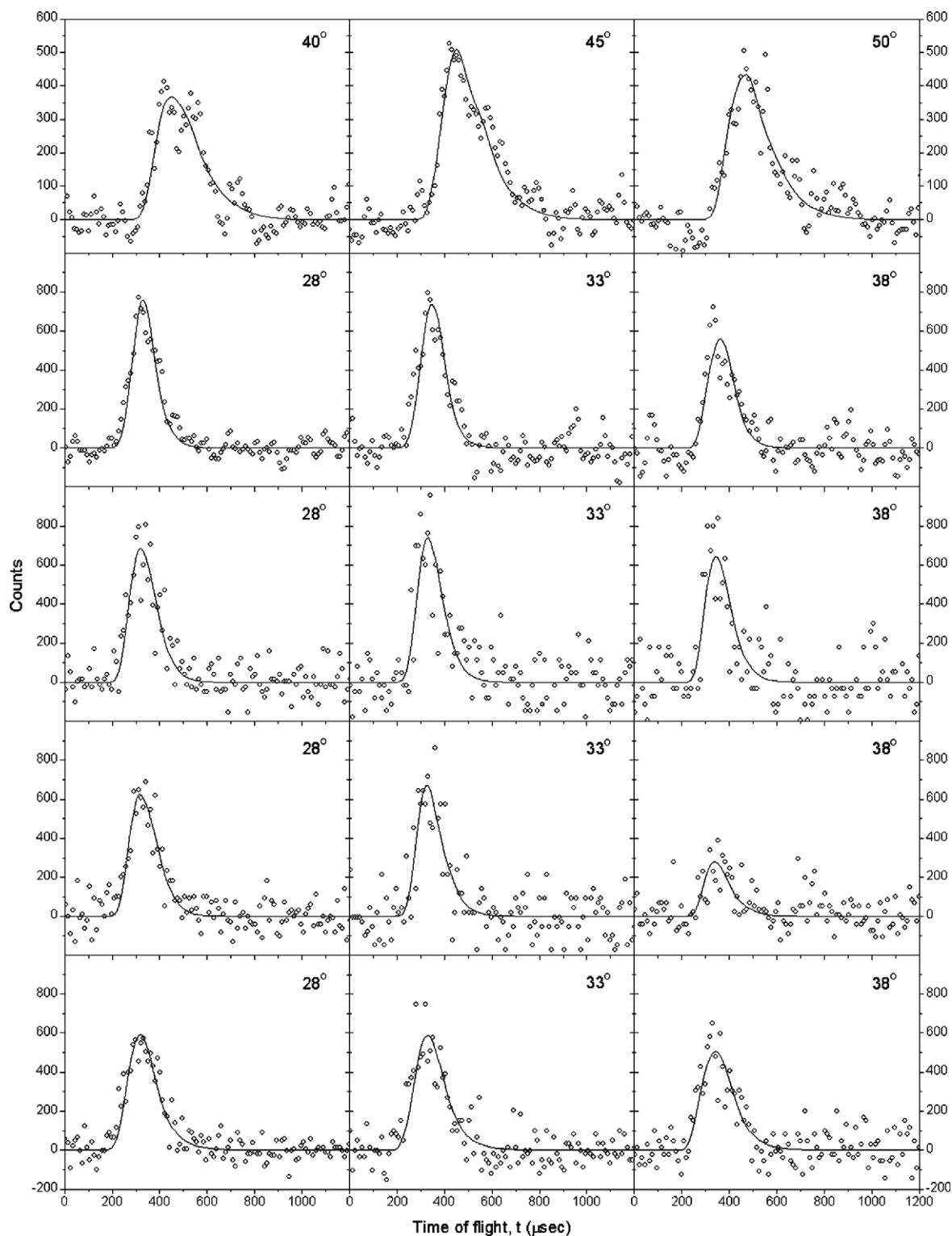


Fig. 2b. Selected time-of-flight data for the reactions of dicarbon with D1-ethylene, *cis*-D2-ethylene, *trans*-D2-ethylene, *gem*-D2-ethylene, and D4-ethylene (top row to bottom row) recorded at $m/z = 52$ ($C_4H_2D^+$) (first row), $m/z = 53$ ($C_4HD_2^+$) (rows two, three, and four), and $m/z = 54$ ($C_4D_3^+$) (lower row). The circles indicate the experimental data, the solid lines the calculated fits.

D2-ethylene isotopomers, i.e. $H_2CCD_2(X^1A_1)$, *trans*- $C_2H_2D_2(X^1A_1)$, and *cis*- $C_2H_2D_2(X^1A_1)$, were carried out at collision energies between 29.1 kJ mol^{-1} and 29.5 kJ mol^{-1} . Finally, we conducted an experiment with D4-

ethylene ($C_2D_4(X^1A_g)$) to compare the life time(s) of the perdeuterated C_4D_4 isotopomers with the corresponding C_4H_4 intermediates. Since the isotopically labeled reactants are very expensive, we restricted ourselves to the detection

of the dicarbon versus atomic hydrogen (C_2H_3D , H_2CCD_2 , $C_2H_2D_2$) and deuterium (C_2D_4) exchange channel. Here, signal was monitored at $m/z = 52$ ($C_4H_2D^+$; C_2H_3D reactant), $m/z = 53$ ($C_4HD_2^+$; $C_2H_2D_2$ reactants), and $m/z = 54$ ($C_4D_3^+$; C_2D_4 reactant). The TOF data and LAB distributions are compiled in Figs. 2b and 3b, respec-

tively. It should be stressed that the LAB distributions obtained in the $C_2H_2D_2$ experiments (*cis*, *trans*, *gem*) are identical within the error limits; likewise, the shape is very similar to the LAB distribution as obtained from the ethylene reactant at a collision energy of 27.8 kJ mol^{-1} . Note that due to the higher mass of the deuterium compared

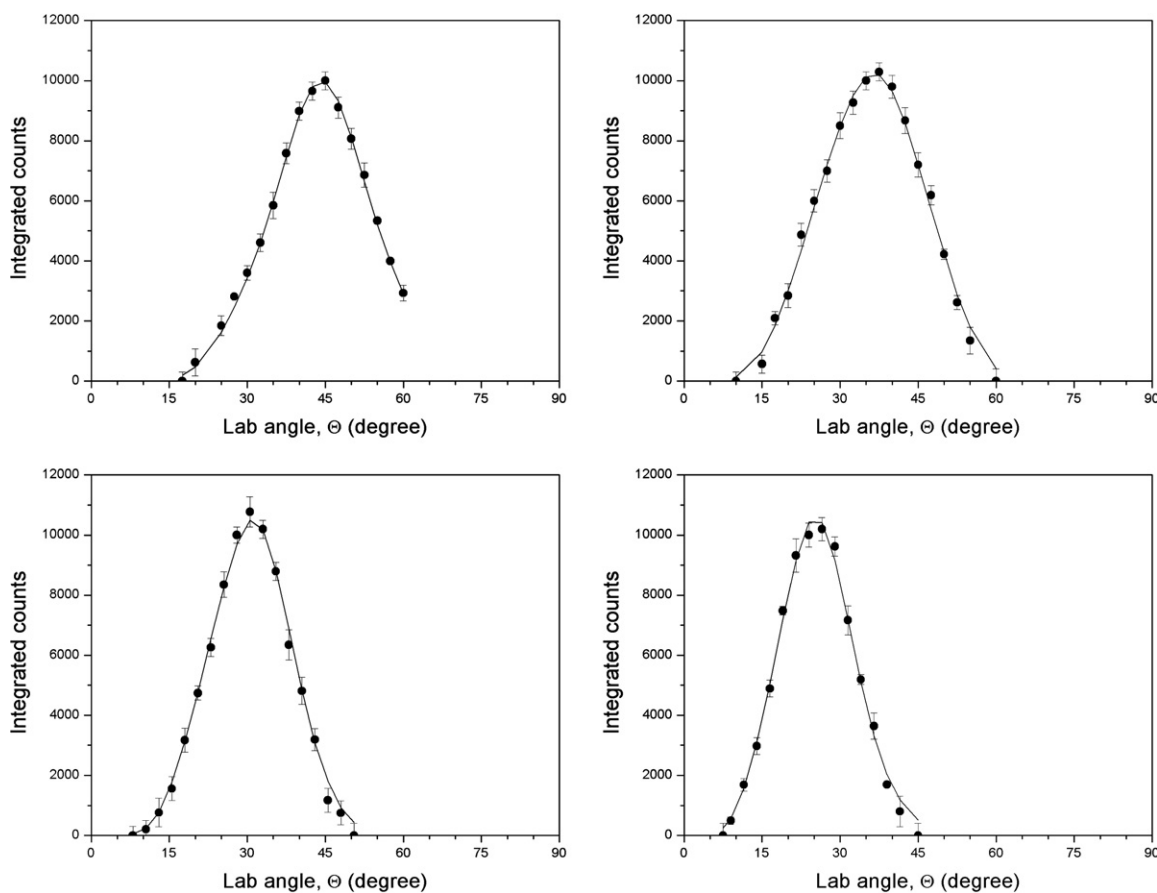


Fig. 3a. Laboratory angular distribution of the C_4H_3 radical(s) recorded at $m/z = 50$ ($C_4H_2^+$) for four collision energies of 12.1 (top left), 19.9 (top right), 30.1 (bottom left), and 40.9 kJ mol^{-1} (bottom right). Circles and error bars indicate experimental data, the solid line the calculated distribution with the best-fit center-of-mass functions.

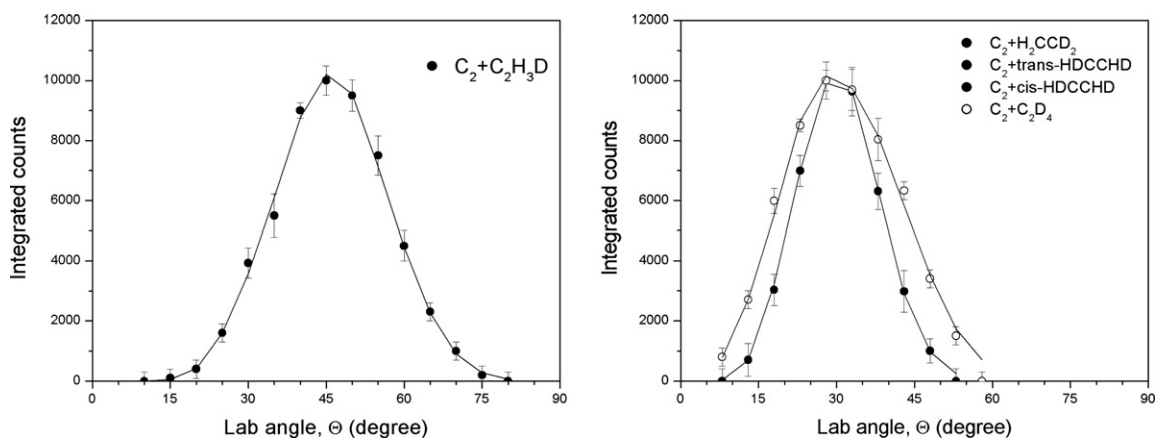


Fig. 3b. Laboratory angular distribution of the C_4H_2D radical recorded at $m/z = 52$ ($C_4H_2D^+$) (left) and of the C_4HD_2 as well as C_4D_3 radicals (both right) recorded at $m/z = 53$ ($C_4HD_2^+$) and $m/z = 54$ ($C_4D_3^+$). The circles indicate the experimental data, the solid lines the calculated fit.

to the hydrogen atom, the LAB distribution of the C_4D_3 product is significantly broader than the distribution of the C_4H_3 product (Figs. 3a and 3b).

3.3. Center-of-mass angular distributions

The translational energy distributions in the center-of-mass-frame, $P(E_T)$, and the center-of-mass angular distributions, $T(\theta)$, are compiled in Fig. 4. We would like to address first the distributions obtained in the reactions of dicarbon plus ethylene. Most important, all distributions exhibit intensity from 0° to 180° . This suggests that the reaction is indirect and involves C_4H_4 complex(es) together with their (partially) deuterated counterparts. As the collision energy increases, the shape of the derived $T(\theta)$ functions changes. At the lowest collision energy of 12.1 kJ mol^{-1} , the $T(\theta)$ is – within the error limits – forward–backward symmetric. The center-of-mass distribution exhibits a pronounced peaking at 90° . This finding could document geometrical constraints of the direction of the atomic hydrogen atom emission in the decomposing

C_4H_4 intermediate(s) at this collision energy [30]. With rising collision energy, the distributions become increasingly backward scattered yielding intensity ratios at the poles, $T(0^\circ)/T(180^\circ)$, of 0.51 ± 0.08 (19.9 kJ mol^{-1}), via 0.40 ± 0.03 (30.1 kJ mol^{-1}) to 0.33 ± 0.03 (40.9 kJ mol^{-1}). The collision energy dependence of the ratios of the center-of-mass angular distributions at the poles could be fit with a decaying function (Eq. (2)) (Fig. 6). The tendency can also be visualized by inspecting the best fit center-of-mass flux contour maps shown in Fig. 5

$$T(0^\circ)/T(180^\circ) = (0.34 \pm 0.05) + (3.0 \pm 2.1) \times e^{-(E_c/(7.7 \pm 2.9))}. \quad (2)$$

Considering the atomic hydrogen loss pathway monitored in the reaction of dicarbon with D1-ethylene ($C_2H_3D(X^1A')$) at a selected collision energy of 12.3 kJ mol^{-1} , it is very interesting to observe that in the C_2/C_2H_3D system, the laboratory data cannot be fit with an identical $T(\theta)$ as obtained in the C_2/C_2H_4 system at a similar collision energy of 12.1 kJ mol^{-1} . First, the peaking at 90° is less obvious. Secondly, the forward–backward-symmetry is broken and the $T(\theta)$ in the C_2/C_2H_3D system is

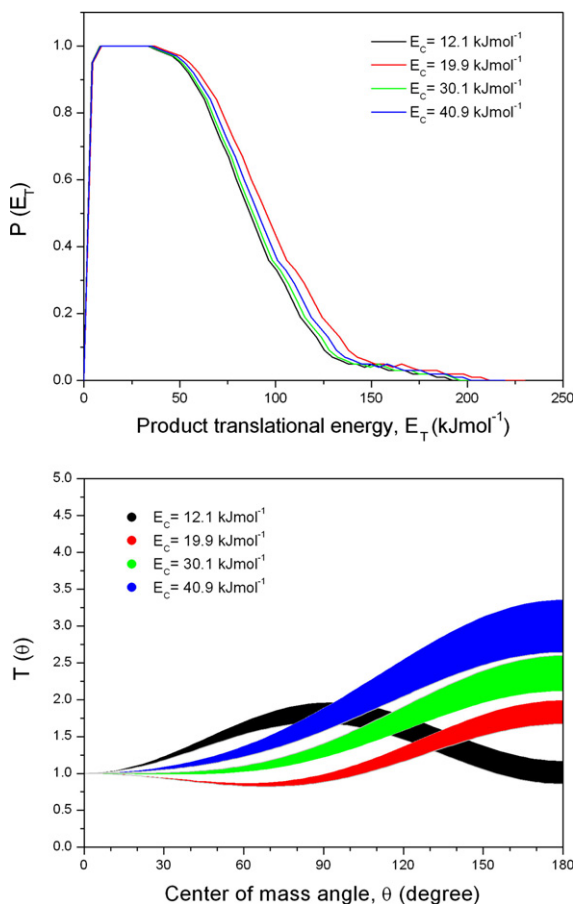


Fig. 4a. Center-of-mass angular (bottom) and translational energy flux distributions (top) for the reaction of dicarbon with ethylene at four collision energies. Regions of identical colors indicate the fits obtained within the error limits of our experiments. (For interpretation of the references to colour in this figure legend, the reader is referred to the web version of this article.)

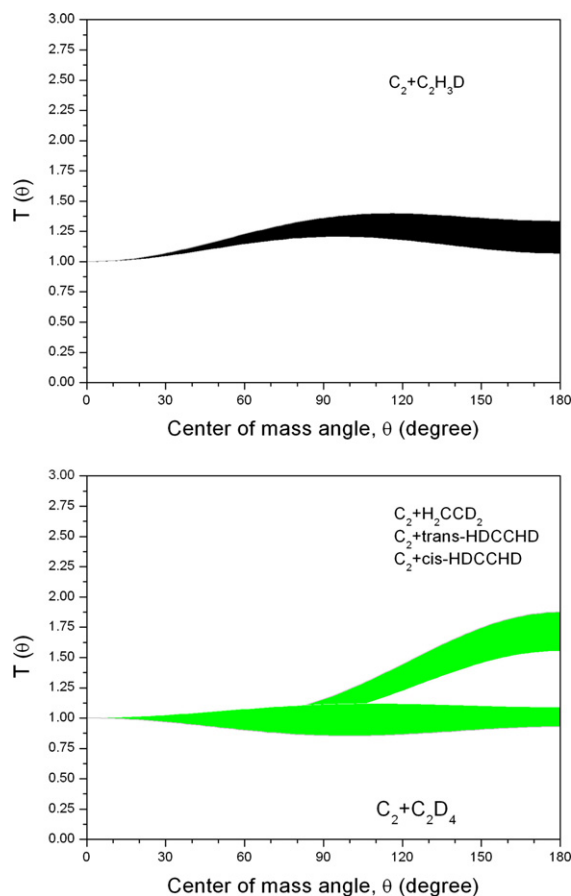


Fig. 4b. Center-of-mass angular distributions of the C_4H_2D radical (top), the C_4HD_2 radical as well as C_4D_3 radicals (both lower). Regions of identical colors indicate the fits obtained within the error limits of our experiments. (For interpretation of the references to colour in this figure legend, the reader is referred to the web version of this article.)

slightly backward scattered compared to the C_2/C_2H_4 system. As expected from the laboratory angular distributions (Fig. 3b), the $T(\theta)$ of the H_2CCD_2 , *trans*- $C_2H_2D_2$, and *cis*- $C_2H_2D_2$, could be fit with identical $T(\theta)$ s. Also, compared to the C_2/C_2H_4 system, the $T(\theta)$ s obtained in the reactions of the D2-substituted ethylene with dicarbon are less backward-scattered. Finally, the $T(\theta)$ extracted from the C_2/C_2D_4 reaction is almost forward–backward symmetric at a collision energy of 31.2 kJ mol^{-1} . This is in strong contrast to the $T(\theta)$ obtained in the C_2/C_2H_4 system which exhibits a pronounced backward-scattering at this collision energy. Summarized, the replacement of (a) hydrogen atom(s) by deuterium has a distinct effect on the shape of the $T(\theta)$ distributions and, hence, on the reaction dynamics. This is in strong contrast to the dicarbon-acetylene sys-

tem studied earlier where no marked differences between the acetylene and isotopically-labeled reactants were found [31]. In Section 4, we will comment on possible explanations to rationalize the experimental findings.

3.4. Center-of-mass translational energy distributions

Fig. 4 exhibits the translational energy distributions in the center-of-mass frame, $P(E_T)$, for the C_2/C_2H_4 reactions at four collision energies. Here, best fits of the LAB distributions and of the TOF spectra were obtained with only one $P(E_T)$ at each collision energy extending to a maximum translational energy, E_{max} , of 191 kJ mol^{-1} ($E_c = 12.1 \text{ kJ mol}^{-1}$), 195 kJ mol^{-1} ($E_c = 19.9 \text{ kJ mol}^{-1}$), 208 kJ mol^{-1} ($E_c = 30.1 \text{ kJ mol}^{-1}$), and 214 kJ mol^{-1} ($E_c = 40.9$

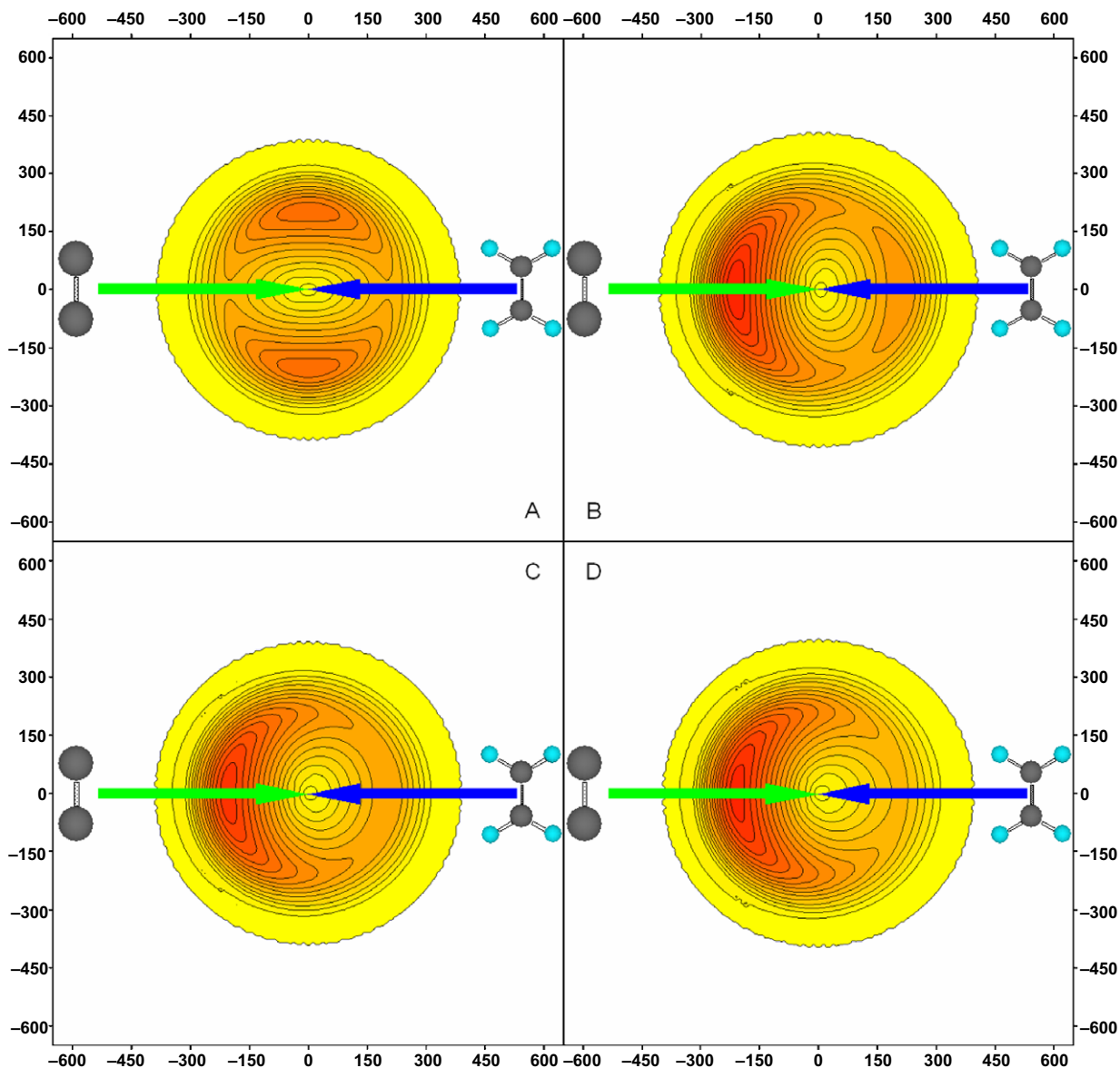


Fig. 5. Center-of-mass flux contour maps of the C_4H_3 radical at four collision energies of 12.1 (A), 19.9 (B), 30.1 (C), and 40.9 kJ mol^{-1} (D). The solid lines connect data with identical fluxes.

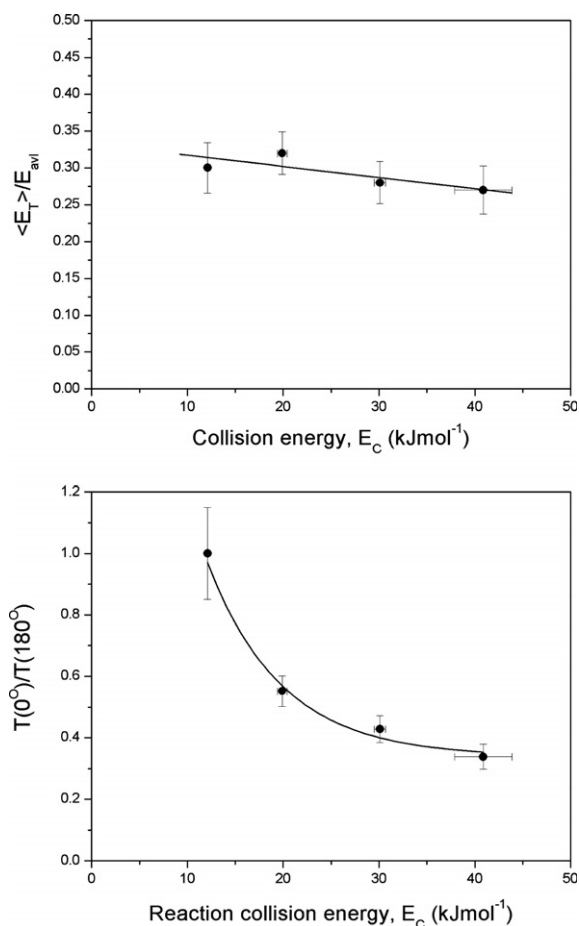


Fig. 6. Collision energy dependence of the fraction of the available energy channeled into the translational modes of the products of the dicarbon-ethylene reaction (top) and of the intensity ratio of the center-of-mass angular distributions at the poles, $T(0^\circ)/T(180^\circ)$.

kJ mol⁻¹). It should be emphasized that because of the emission of a light hydrogen atom, the derived fits are relatively insensitive to the high energy cut-off. Here, extending or cutting the tail by about 10 kJ mol⁻¹ did not influence the quality of the fit. Considering those molecules without internal excitation, the maximum translational energy is simply the collision energy plus the reaction energy. Therefore, E_{max} helps in calculating the reaction exoergicity. Averaging over all four collision energies, we find that the formation of the C_4H_3 radical(s) and atomic hydrogen is exoergic by 176 ± 10 kJ mol⁻¹. We have to recall that the dicarbon reactant is in its $X^1\Sigma_g^+$ electronic ground and in its first excited $a^3\Pi_u$ state. Therefore, the reaction with the triplet state is more exoergic by 8.6 kJ mol⁻¹ compared to the singlet reactant. Therefore, we have to conclude that the reaction of $\text{C}_2(X^1\Sigma_g^+)$ with ethylene to form C_4H_3 radical(s) and atomic hydrogen is exoergic by 167 ± 10 kJ mol⁻¹.

Besides the high-energy cutoff, it should be noted that in the most favorable case, the most probable translational energy represents an order-of-magnitude of the barrier height in the exit channel. Here, all $P(E_T)$ s show broad pla-

teaus between 5 kJ mol⁻¹ and about 45 kJ mol⁻¹. These data indicate that at least one reaction channel exhibits most likely an exit barrier. Also, the peaking of the $P(E_T)$ at lower collision energies close to zero translation energy might indicate the existence of a second reaction pathway which involves almost no exit barrier and hence a loose exit transition state [31]. Secondly, based on the center-of-mass translational energy distributions, we can estimate the fraction of the energy channeling into the translational modes of the products, E_T/E_{av} (Fig. 6). As the collision energy rises, the averaged fraction of the translational energy is reduced from about $32 \pm 3\%$ to $26 \pm 4\%$. This order of magnitude of about 30%, which is almost independent on the collision energy, suggests that the reaction dynamics are indirect – in close agreement with the shape of the center-of-mass angular distributions (Section 3.2). Finally, we would like to stress that the TOF spectra (Fig. 2) and LAB distributions (Fig. 3) of the isotopically labeled reaction products could be fit – within the error limits – with identical center-of-mass translational energy $P(E_T)$ distributions as derived from the $\text{C}_2/\text{C}_2\text{H}_4$ system at similar collision energies.

4. Discussion

The detailed analysis of the center-of-mass translational energy distributions implies that the reaction of singlet dicarbon with ethylene to form C_4H_3 radical(s) plus a hydrogen atom is exoergic by 167 ± 10 kJ mol⁻¹ (Section 3.3). Based on the energetics, we compute the enthalpy of formation of the C_4H_3 species formed to be 504 ± 10 kJ mol⁻¹. We would like to comment briefly on the reference temperature. Since, the reactants are formed in a supersonic expansion, we can approximate that the rotation and vibrational temperatures of the reactant molecules are a few 10 K. Therefore, we can neglect the entropy factor, and the reaction energy is almost identical to the reaction enthalpy. We can contrast then the experimentally derived enthalpy of formation with computed data at 0 K. Our experimental data compare nicely with the computed enthalpies of formation of the $i\text{-C}_4\text{H}_3(X^2A')$ isomer (Fig. 1), i.e. in the range of 498–499 kJ mol⁻¹ [12–14]. The formation of the corresponding $n\text{-C}_4\text{H}_3(X^2A')$ isomer, which is less stable by 28–48 kJ mol⁻¹ [12–14], cannot account for the experimentally derived enthalpy of formation. The conclusion of the formation of the $i\text{-C}_4\text{H}_3(X^2A')$ isomer agrees well with a computational study in the limits of a statistical energy distribution predicting that the $n\text{-C}_4\text{H}_3(X^2A')$ isomer should be formed to less than 1% [20,21]. The shape of the $P(E_T)$ s and the inherent broad plateaus extending to 45 kJ mol⁻¹ (Section 3.2), are indicative of a reaction involving two channels [31]: one with an exit barrier and a second barrier-less pathway to form the $i\text{-C}_4\text{H}_3(X^2A')$ isomer. An inspection of the singlet PES (Fig. 7) indicates only three barrier-less pathways to the reaction product. The triplet surface exhibits two exit channels to the $i\text{-C}_4\text{H}_3(X^2A')$ isomer; both pathways have to go

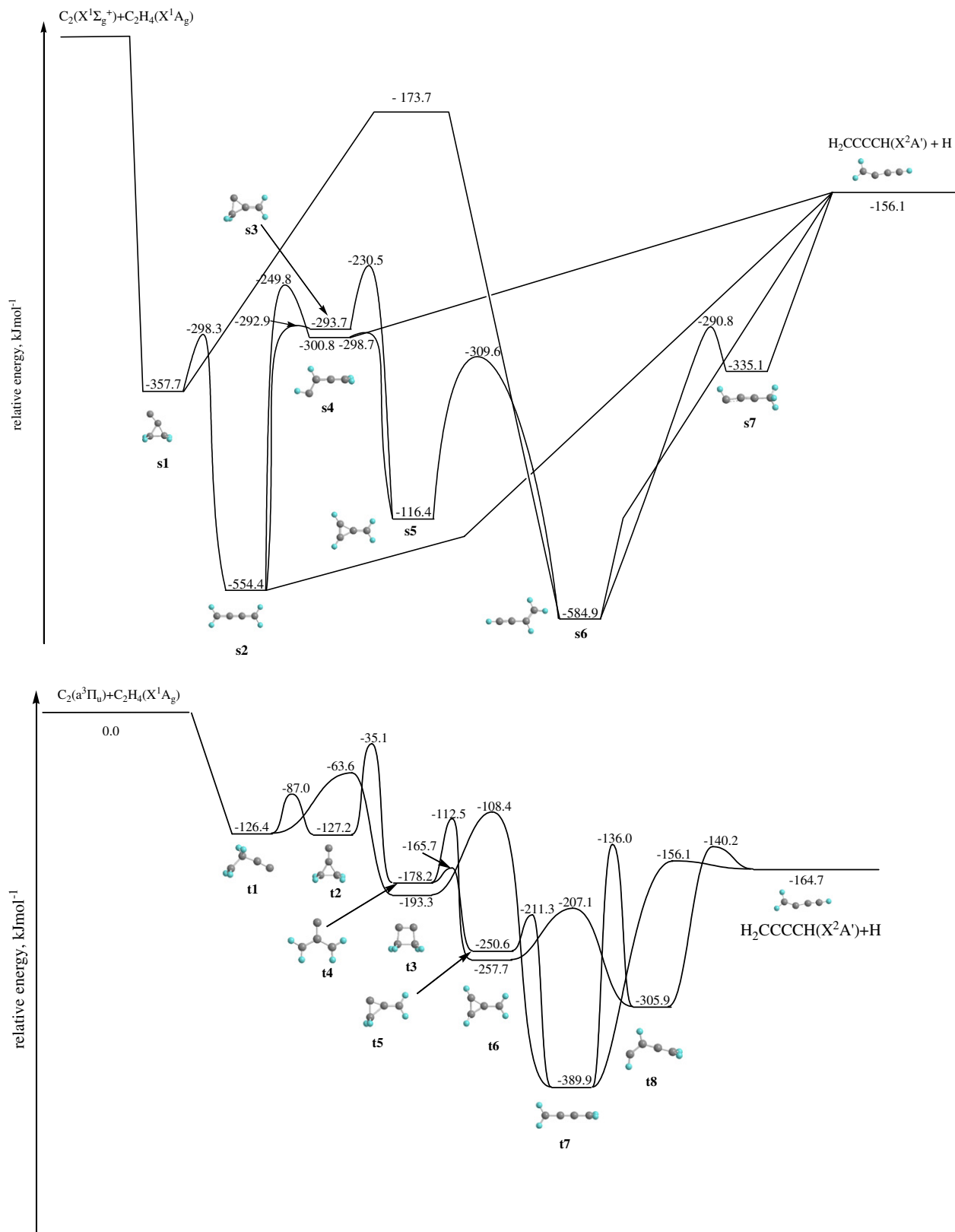


Fig. 7. Simplified singlet (top) and triplet (bottom) potential energy surfaces involving atomic hydrogen loss pathways in the reaction of dicarbon, $C_2(X^1\Sigma_g^+/a^3\Pi_u)$, with ethylene to form i - C_4H_3 extracted from Refs. [21,22].

through tight exit transition states starting with intermediates **t7** and **t8**.

We would like to address briefly the non-detection of the molecular hydrogen pathway. Within the RRKM limits

[21], the computations suggest that the molecular hydrogen channel should be present at a level of about 14% relative to the atomic hydrogen pathway. However, various possibilities could exist why we do not observe this pathway. First, dynamical (non-statistical) effects could favor the hydrogen atom loss compared to the molecular hydrogen elimination pathway. In this case, the RRKM calculations would effectively overestimate the importance of the molecular hydrogen channel. Alternatively, we should recall that we do not know the *relative* abundance of triplet versus singlet dicarbon in our beam (Section 2); hence, even if our beam contains a 1:1 ratio of triplet versus singlet dicarbon, this would push the fraction of the molecular hydrogen level to about 7% – close to the sensitivity limit of our fits. Here, an inclusion of up to 5% of the $C_4H_2 + H_2$ pathway does not influence the quality of the TOF and LAB fits at $m/z = 50$.

Now, we attempt to investigate how the changes in the shapes of the center-of-mass angular distributions (Fig. 4) with the collision energy (together with the inherent life time of the decomposing intermediate) and by replacing hydrogen by deuterium can be rationalized. Let us consider the C_2/C_2H_4 system first. Most importantly, the sole existence of a singlet butatriene intermediate cannot account for the experimentally found asymmetry in the center-of-mass angular distributions at collision energies of 19.9 kJ mol^{-1} and higher. Considering angular momentum conservation, each reaction intermediate must be excited to A, B, and/or C like rotations. Since singlet butatriene belongs to the D_{2h} point group, a C_2 axis is parallel to each principal rotational axis. This in turn classifies the butatriene intermediate as ‘symmetric’; each C_2 rotational axis can therefore inter convert the dissociating hydrogen atom giving this atom an equal probability to leave in a direction of θ° or $\pi - \theta^\circ$. Consequently, the center-of-mass angular distribution would be always forward–backward symmetric at all collision energies – although the life-time of the intermediate might be less than its rotation period – if only singlet butatriene is the decomposing intermediate. This has clearly not been observed experimentally. Therefore, we have to conclude that there must be a second intermediate which decomposes to the $i\text{-}C_4H_3(X^2A')$ isomer via an atomic hydrogen loss. On the triplet surface (recall that based on the $P(E_T)$ s, the triplet surface must be involved in the underlying dynamics), the situation is intriguing. Triplet butatriene (point group: D_{2d}) only holds a twofold rotational parallel to the A principal axis. Therefore, only if triplet butatriene is excited to A-like rotations, the center-of-mass angular distribution will be forward–backward symmetric. Note that there are two additional C_2 -axes intersecting the plane spanned by the B and C-axes at an angle of 45° . However, it should be stressed that these axes are not parallel to any rotational axis, and can therefore not be considered. Therefore, triplet butatriene (**t7**) excited to B/C like rotations could account for the asymmetry of the center-of-mass angular distributions at higher collision energies. As a matter of fact, this intermediate was identi-

fied – based on the $P(E_T)$ s – as one of the decomposing complexes leading to $i\text{-}C_4H_3(X^2A')$ plus atomic hydrogen via a tight exit transition state. Considering the barriers involved in the isomerization of **t7**–**t8**, and comparing this number with the barrier of the atomic hydrogen loss from **t7** (about 9 kJ mol^{-1}) (Fig. 7), we expect that **t7** rather dissociates via hydrogen atom loss rather than undergoing an isomerization to **t8**. This has been confirmed computationally [20]. A second pathway to **t8** might involve the reaction sequence **t1** → **t2** → **t4** → **t6** → **t8**. However, the transition state involved in the **t2** → **t4** isomerization is energetically unfavorable compared to the **t2** → **t1** step followed by **t3** → **t7**. Therefore, we can conclude that **t7** is the predominant decomposing intermediate on the triplet surface, which can account for the off-zero-peaking of the translational energy distributions and also for the asymmetry – once rotating around the B/C axes – of the center-of-mass angular distributions at higher collision energies. The enhanced asymmetry could be explained in terms of a shorter life time as the collision energy increases. However, could there be also an ‘asymmetric’ intermediate on the singlet surface? Note that besides singlet butatriene (**s2**), **s6** and **s7** – both asymmetric intermediates – could also decompose to $i\text{-}C_4H_3(X^2A') + H(S_{1/2})$. The structures are accessible via **s1** → **s6** and the multi step **s1** → **s2** → **s3/s4** → **s5** → **s6** → **s7** sequence. The first option can be likely ruled out since the involved barrier (316 kJ mol^{-1}) compared to the ring-opening of **s1** to singlet butatriene (59 kJ mol^{-1}). Therefore, only the multi-step reaction sequence can lead to **s6/s7**. Considering the non-detection of the molecular hydrogen elimination pathway – which has to go through **s7** – we can likely eliminate **s7** as a major contributor to the asymmetry of the center-of-mass angular distributions at higher collision energies. Therefore, we can conclude that triplet butatriene rotating around B/C axes is likely the dominant intermediate giving rise to an asymmetry of the center-of-mass angular distributions at higher collision energies; however, we acknowledge that minor contributions from **s6/s7** cannot be ruled out completely.

Finally, it is important to link the deuterium labeled experiment to the previous discussion. First, we would like to compare the C_2/C_2H_4 with the C_2/C_2H_3D system at collision energies of 12.1 and 12.3 kJ mol^{-1} . Recall that the original goal was to reduce the symmetry of the singlet butatriene intermediate from D_{2h} to C_s . Therefore, this procedure is expected to help elucidating to what extent the forward–backward symmetric center-of-mass angular distribution in the C_2/C_2H_4 system is the effect of the symmetry of the butatriene intermediate or solely from a long-lived complex behavior. We observe that within the error limits, both the C_2/C_2H_4 with the C_2/C_2H_3D systems can be fit with a forward–backward symmetric center-of-mass angular distribution. Hence, we have to conclude that at the lowest collision energy of 12.1 kJ mol^{-1} , the life time of the singlet/triplet butatriene intermediates is truly longer than their rotation period. We realized that the peaking of the distribution at 90° in the C_2/C_2H_3D system is less

pronounced than in the reaction of dicarbon with ethylene. This could be the result – due to the distinct mass combinations of the products – of a different coupling of the initial angular momentum into the rotational degrees of freedom of the final reaction products in both systems. Sec-

only, we present an assessment of the *gem*-, *cis*-, and *trans*- $C_2/C_2H_2D_2$ reactions and compare these findings with the C_2/C_2H_4 system. Recall that all data in the *gem*-, *cis*-, and *trans*- $C_2/C_2H_2D_2$ systems could be fit with *identical* center-of-mass functions. If we transfer the proposed

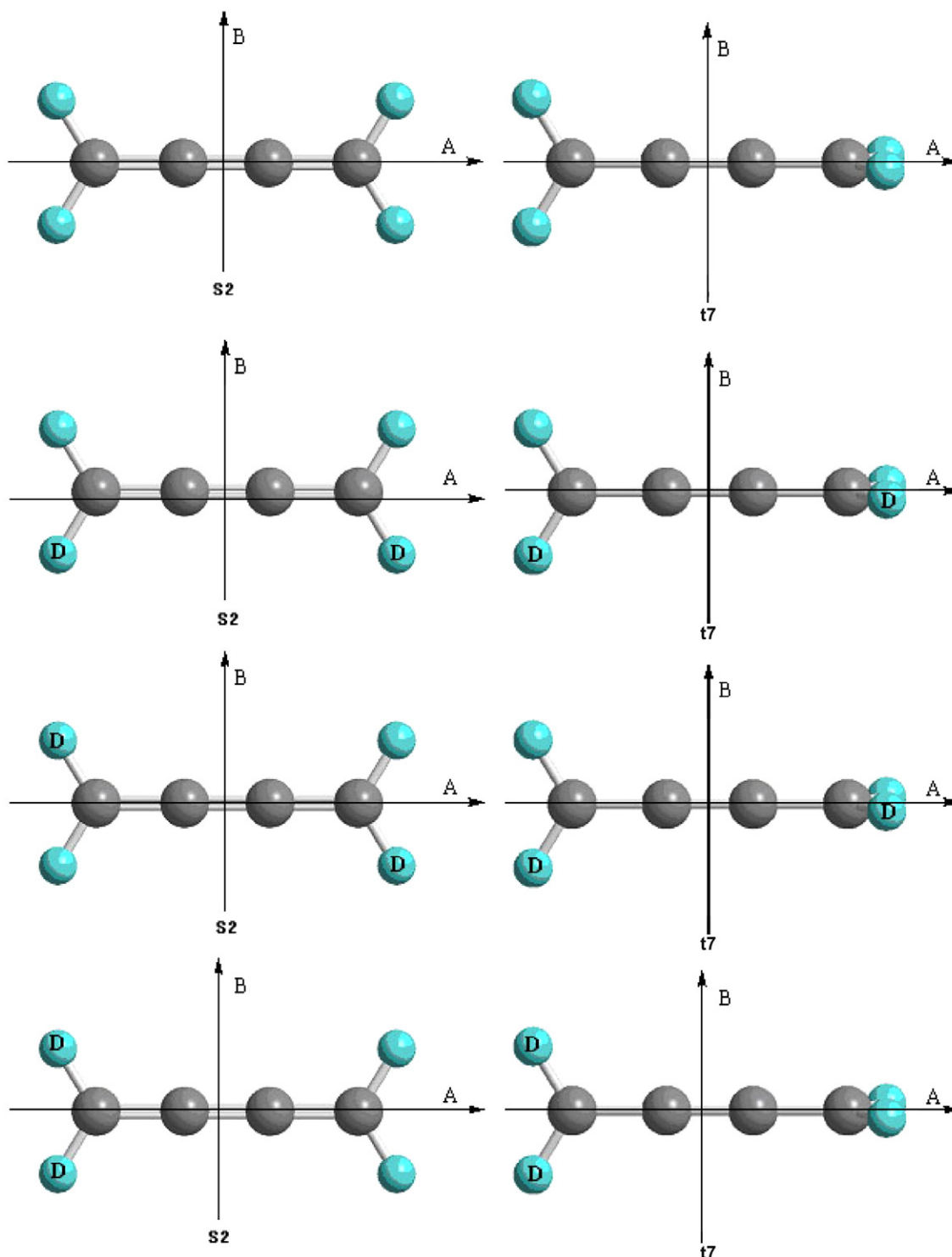


Fig. 8. Rotational axis and structures of singlet and triplet butatriene (upper row), and D₂-butatriene intermediates (second row: reaction from *cis*-D₂-ethylene; third row: reaction from *trans*-D₂-ethylene; bottom row: reaction from *gem*-D₂-ethylene).

Table 2

Statistical rate constants (s^{-1}) and life times (ps) for the H and D loss from singlet (**s2**) and triplet (**t7**) butatriene and their D2 and D4 isotopomers, calculated for the collision energy of 31.4 kJ mol^{-1} in the limit of a statistical energy randomization

Singlet	C ₄ H ₄	H ₂ C ₄ D ₂		HDC ₄ HD <i>trans</i>		HDC ₄ HD <i>cis</i>		C ₄ D ₄
	H loss	H loss	D loss	H loss	D loss	H loss	D loss	D loss
<i>k</i>	5.57×10^9	1.85×10^9	1.36×10^9	1.99×10^9	1.30×10^9	2.01×10^9	1.28×10^9	1.84×10^9
$k_{\text{H}} + k_{\text{D}}$	5.57×10^9	3.21×10^9		3.29×10^9		3.28×10^9		1.84×10^9
Life time	179.5	311.4		303.8		304.7		542.2
Triplet	C ₄ H ₄	H ₂ C ₄ D ₂		HDC ₄ HD		C ₄ D ₄		
	H loss	H loss	D loss	H loss	D loss	D loss		
<i>k</i>	2.67×10^{11}	1.07×10^{11}	6.16×10^{10}	1.10×10^{11}	6.01×10^{10}	9.57×10^{10}		
$k_{\text{H}} + k_{\text{D}}$	2.67×10^{11}	1.69×10^{11}		1.70×10^{11}		9.57×10^{10}		
Life time	3.7	5.9		5.9		10.5		

reaction mechanisms of the C₂/C₂H₄ system on the singlet (**s1** → **s2** → *i*-C₄H₃(X²A') + H(²S_{1/2})) and triplet (**t1** → **t3** → **t7** → *i*-C₄H₃(X²A') + H(²S_{1/2})) surfaces to distinct C₂H₂D₂ isotopomers, we expect the formation of the D2-substituted butatriene intermediates as compiled in Fig. 8. The D2-isotopomers resulting from the *cis*- and *trans*-C₂H₂D₂ reactants are identical on the triplet surface and belong both to the C_s point group. On the singlet surface, the C_{2v} and D_{2h} structures can be classified as symmetric intermediates if they are excited to B and C-like rotations, respectively. Therefore, decomposing complexes on the singlet surface can still result in a forward–backward symmetric center-of-mass angular distribution; the asymmetry of the *T*(θ)s likely originates from the triplet surface. Since both intermediates are identical, this would result in identical center-of-mass functions as derived from the experimental data. The reaction of dicarbon with *gem*-C₂H₂D₂ shows explicitly that D2-butatriene intermediates cannot be excited to A-like rotations. Both on the triplet and singlet surface, the intermediates belong to the C_{2v} point group holding a twofold rotation axis parallel to the A principal rotation axis. Here, a rotation around the A axis would result in a forward–backward center-of-mass angular distribution both from the singlet and the triplet surface. Clearly, this has not been observed experimentally, and we can conclude again that the butatriene intermediates are most likely excited to B/C like rotations. We would like to stress that the *T*(θ)s in the C₂/C₂H₂D₂ systems are less asymmetric as compared to the C₂/C₂H₄ reaction. Recall that all systems have been studied at collision energies of 30.1–31.2 kJ mol⁻¹. This could be an effect of the substitution of two hydrogen atoms by two deuterium atoms and the inherent reduction of the frequency of the C–D bending and stretching modes compared to C–H. This would result in an enhanced life time of the intermediates. Our statistical computations confirm this (see Table 2). We find longer life times with respect to hydrogen and deuterium loss for the singlet and triplet D2-butatriene intermediates (304–311 ps and 6 ps, respectively) as compared to 180 ps and 4 ps, respectively, in the case of singlet and triplet butatriene. This trend is amplified in the C₂/

C₂D₄ system, which shows a forward–backward symmetric center-of-mass angular distribution. Here, we find life times of the singlet and triplet D4-butatriene of 542 ps and 11 ps, respectively. Again, these life times are longer than the corresponding singlet and triplet butatriene intermediates at a similar collision energy.

5. Conclusions

We examined the chemical dynamics of the formation of the *i*-C₄H₃(X²A') radical together with its (partially) deuterated isotopomers in eight crossed molecular beams experiments of dicarbon molecules in their X¹Σ_g⁺ electronic ground and in its first excited a³Π_u state with (partially deuterated) ethylene at collision energies between 12.1 and 40.9 kJ mol⁻¹. First, our experiments helped to determine the enthalpy of formation of the *i*-C₄H₃(X²A') radical to be about $504 \pm 10 \text{ kJ mol}^{-1}$ in good agreement with previous computational studies suggesting 498–499 kJ mol⁻¹. Secondly, the collision-energy dependence of the center-of-mass angular distributions suggests that the reaction dynamics on the singlet and triplet surfaces are indirect and involve butatriene reaction intermediates. In case of the C₂/C₂H₄ reaction, the ‘symmetric’ singlet butatriene intermediate would lead solely to a symmetric center-of-mass angular distribution; however, in combination with isotopically labeled reactants, we concluded that triplet butatriene intermediates excited to B/C like rotations likely account for the observed asymmetries in the center-of-mass angular distributions at higher collision energies. The translational energy distributions are also indicative of the involvement of both the triplet and singlet surfaces which lead both to the *i*-C₄H₃(X²A') radicals through lose (singlet) and tight (triplet) exit transitions states. The explicit identification of the resonance-stabilized *i*-C₄H₃(X²A') radical also suggests that the reaction of dicarbon with ethylene can lead to formation of this radical in combustion flames; however, the *n*-C₄H₃(X²A') isomer is not formed in the title reaction. This conclusion correlates nicely with Hansen’s et al. flame experiments observing only the *i*-C₄H₃(X²A') radical in hydrocarbon flames [14].

Acknowledgements

The experimental and theoretical work was supported by the US Department of Energy-Basic Energy Sciences (DE-FG02-03ER15411 and DE-FG02-04ER15570, respectively).

References

- [1] Faraday Discussion 119, combustion chemistry: elementary reactions to macroscopic processes (2001).
- [2] M. Frenklach, *Phys. Chem. Chem. Phys.* 4 (2002) 2028.
- [3] C.E. Baukal, *Oxygen-enhanced Combustion*, CRS Press, New York, 1998.
- [4] A.M. Nienow, J.T. Roberts, *Annu. Rev. Phys. Chem.* 57 (2006) 4.
- [5] M.F. Budyka, T.S. Zyubina, A.G. Ryabenko, V.E. Muradyan, S.E. Esipov, N.I. Cherepanova, *Chem. Phys. Lett.* 354 (2002) 93.
- [6] Y.-T. Lin, R.K. Mishra, S.-L. Lee, *J. Phys. Chem. B* 103 (1999) 3151.
- [7] H. Yang, H. Wang, X. Ran, Q. Shi, Z. Wen, *Theochem* 618 (2002) 209.
- [8] J.D. Bittner, J.B. Howard, *Proc. Comb. Inst.* 18 (1981) 1105.
- [9] M. Frenklach, D.W. Clary, W.C. Gardiner, S.E. Stein, *Proc. Combust. Inst.* 20 (1985) 887.
- [10] (a) A.M. Mebel, in: K.D. Sen (Ed.), *Reviews of Modern Quantum Chemistry*, World Scientific, Singapore, 2002, p. 340;
(b) V.V. Kislov, T.L. Nguyen, A.M. Mebel, S.H. Lin, S.C. Smith, *J. Chem. Phys.* 120 (2004) 7008.
- [11] S.J. Klippenstein, J.A. Miller, *J. Phys. Chem. A* 109 (2005) 4285.
- [12] X. Krokidis, N.W. Moriarty, W.A. Lester, M. Frenklach, *Int. J. Chem. Kinetics* 33 (2001) 808.
- [13] S.E. Wheeler, W.D. Allan, H.F. Schaefer, *J. Chem. Phys.* 121 (2004) 8800.
- [14] N. Hansen, S.J. Klippenstein, C.A. Taatjes, J.A. Miller, J. Wang, T.A. Cool, B. Yang, R. Yang, L. Wei, C. Huang, J. Wang, F. Qi, M.E. Law, P.R. Westmoreland, *J. Phys. Chem. A* 110 (2006) 3670.
- [15] R.I. Kaiser, A.M. Mebel, A.H.H. Chang, S.H. Lin, Y.T. Lee, *J. Chem. Phys.* 110 (1999) 10330.
- [16] R.I. Kaiser, D. Stranges, Y.T. Lee, A.G. Suits, *J. Chem. Phys.* 105 (1996) 8721.
- [17] R.I. Kaiser, F. Stahl, P.v.R. Schleyer, H.F. Schaefer, *Phys. Chem. Chem. Phys.* 13 (2002) 950;
T.L. Nguyen, A.M. Mebel, S.H. Lin, R.I. Kaiser, *J. Phys. Chem. A* 105 (2001) 115498.
- [18] R.I. Kaiser, W. Sun, A.G. Suits, Y.T. Lee, *J. Chem. Phys.* 107 (1997) 8713.
- [19] N. Balucani, A.M. Mebel, Y.T. Lee, R.I. Kaiser, *J. Phys. Chem. A* 105 (2001) 9813.
- [20] X. Gu, Y. Guo, F. Zhang, A.M. Mebel, R.I. Kaiser, *Faraday Discuss.* 133 (2006) 245.
- [21] A.M. Mebel, V.V. Kislov, R.I. Kaiser, *J. Chem. Phys.* 125 (2006) 133113.
- [22] R.I. Kaiser, C. Ochsenfeld, M. Head-Gordon, Y.T. Lee, A.G. Suits, *Science* 274 (1996) 1508.
- [23] X. Gu, Y. Guo, R.I. Kaiser, *Int. J. Mass Spectr.* 246 (2005) 29.
- [24] X. Gu, Y. Guo, E. Kawamura, R.I. Kaiser, *J. Vac. Sci. Technol. A* 24 (2006) 505.
- [25] R.I. Kaiser, Y. Osamura, *J. Phys. Chem. A* 106 (2002) 4825.
- [26] R.I. Kaiser, A.M. Mebel, N. Balucani, Y.T. Lee, F. Stahl, P.v.R. Schleyer, H.F. Schaefer, *Faraday Discuss.* 119 (2001) 51.
- [27] R.I. Kaiser, D. Stranges, Y.T. Lee, A.G. Suits, *J. Chem. Phys.* 105 (1996) 8721.
- [28] M.S. Weiss, PhD Thesis, 1986, University of California, Berkeley.;
M. Vernon, PhD Thesis, 1981, University of California, Berkeley;
R.I. Kaiser, C. Ochsenfeld, D. Stranges, M. Head-Gordon, Y.T. Lee, *Faraday Discuss.* 109 (1998) 183.
- [29] Y. Guo, X. Gu, R.I. Kaiser, *Int. J. Mass Spectro.* 249–250 (2006) 420.
- [30] It should be outlined that the center-of-mass distribution at lower collision energy obtained from our earlier study of this reaction (Ref. [19]) differ from the present study. Since both data sets were recorded with different ablation source geometries, distinct laser powers, and parts of the pulsed ablation beam, it is likely that the dicarbon beams in both studies have different ratios of singlet versus triplet dicarbon. This may affect the relative contribution of the scattering signal to the micro channels originating from the singlet and triplet surfaces (Ref. [31]).
- [31] X. Gu, Y. Guo, A.M. Mebel, R.I. Kaiser, *J. Phys. Chem. A* 110 (2006) 11265.